

1. Measurement of the light cone angle

The medical team measured the angle of the device by focusing the beams on paper and measuring the distance from the device. They found that the two points coincided at a distance of 12.2 cm from the device's glass. At a distance of about 7 cm, the distance between the centers of the two beams was a centimeter (Fig. 1), and at a distance of about 17 cm, again the distance between the beams was found to be 1 cm.

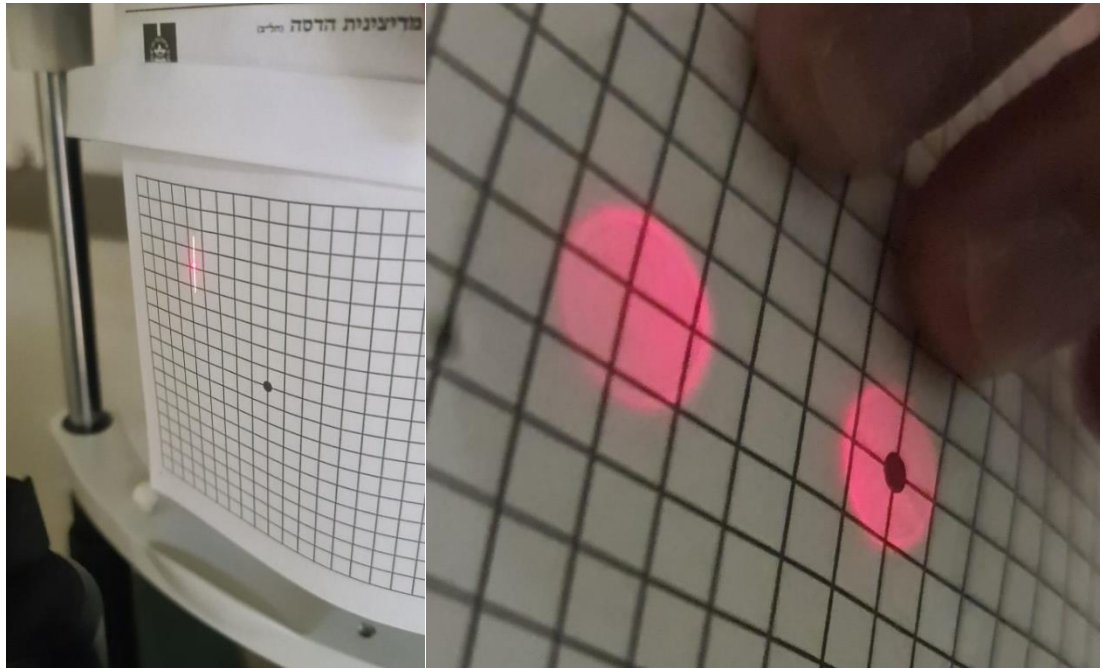


Fig. 1

The measurement conditions were somewhat unstable leading to some uncertainty in the values determined. However, based on the values quoted, the angle was estimated to be 11-12 degrees, which contradicts the technical specifications listed on the device, stating that the cone angle is 16 degrees. According to the medical team, this specification does not refer to the angle they are measuring.

Therefore, there was a need for more accurate measurement, and results were obtained using 3 methods:

- a. The distance between the centers of the two beams was measured at 4 different locations, and the distance from the device to the same plane was recorded. The data was plotted on a graph, and the slope obtained corresponded to an angle of 11 degrees.
- b. A page was placed in the plane of the beams, and the course of the beams along the paper was determined by drawing the centers of the beams on the paper. The measured angle was found to be 12 degrees based on the lines drawn.

- c. The beams that were obtained on the page were photographed (Fig. 2 : aiming beam). The results were analyzed with an angle meter, and it was found that the angle between the outer beams is 16 degrees, and between the centers of the beams it is 12 degrees .

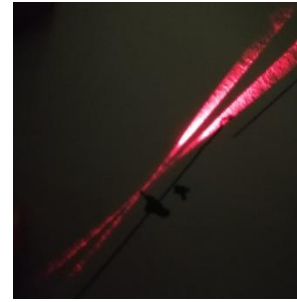


Fig. 2 : aiming beam

A match was found between the angle of the centers of the beams measured in the third method and the angle of the beams measured in the second method, which is 12 degrees. According to the third method, it is possible to understand the record in the technical specifications of the laser, which states that the cone angle is 16 degrees. Therefore, it is possible that the reference is to the external angle of the beams since the beams have a Gaussian profile and as explained in the background, they diverge as they move away from their focal point.

2. Extrapolation of Measured Chromatic Aberration to NIR

The index of refraction and focal length of a typical lens composed of a typical lens glass, BK-7, asymptote to a constant at long wavelengths. The deviation, or derivative decreases to zero. The deviation between 635 and 1064 is less than the deviation over the visible range. (The general form of the curve is of interest here, hence the radius chosen, and the numerical values of f are not great importance here; the graph shows the focal length normalized by its value at the sodium D-line.)

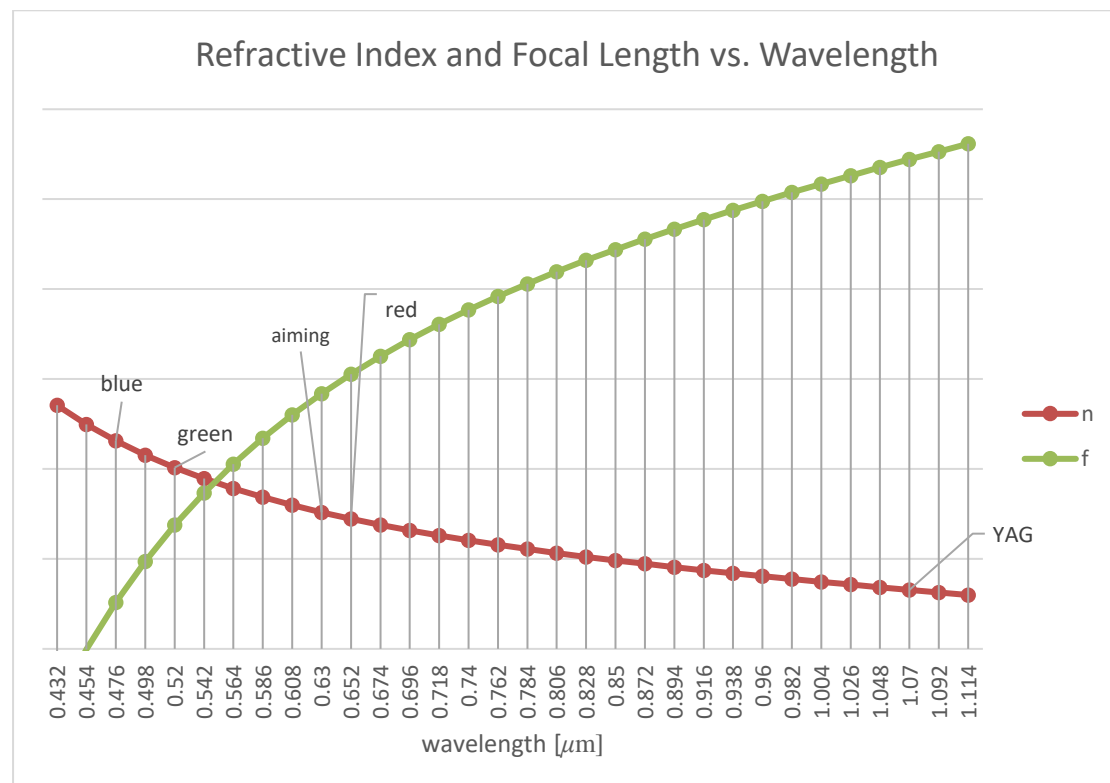


Fig. 3

The comparison is aided by the following table:

| Wavelength [nm] | Color | n | f |
|--------------------|----------------|----------|----------|
| 476 | Blue | 1.523133 | 1.505165 |
| 520 | Green | 1.52016 | 1.513769 |
| 630 | Guide- beam | 1.515186 | 1.528384 |
| 652 | Red | 1.514457 | 1.53055 |
| 1070 | YAG | 1.506556 | 1.554422 |

Table 1

3. Modeling the rays by software

The following are the parameters used to simulate the eye including the auxiliary lens and the ophthalmic lens:

| | Surface Type | Comment | Radius | Thickness | Material | Par 1 (unused) | Coating | Clear Semi-Dia | Chip Zo | Mech Semi-Dia | Conic | TCE x 1E-6 | Par 2 (unused) |
|----|---------------|----------|----------|-----------|------------|----------------|---------|----------------|---------|---------------|---------|------------|----------------|
| 0 | OBJECT (aper) | Standard | Infinity | Infinity | | | | 0.0000000 U | 0.00... | 0.0000000 | 0.00... | 0.0000... | |
| 1 | (aper) | Standard | Infinity | 5.000... | | | | 15.0000000 U | 0.00... | 15.0000000 | 0.00... | 0.0000... | |
| 2 | | Standard | Infinity | 0.000... | | | | 15.0000000 U | 0.00... | 15.0000000 | 0.00... | 0.0000... | |
| 3 | | Standard | Infinity | 0.000... | | | | 15.0000000 U | 0.00... | 15.0000000 | 0.00... | 0.0000... | |
| 4 | STOP (aper) | Paraxial | קונוס | 0.000... | | 120.00000... | | 12.5000000 U | - | - | - | 0.0000... | 1 |
| 5 | | Standard | מרוק | Infinity | 115.1... V | | | 12.5000000 U | 0.00... | 12.5000000 | 0.00... | 0.0000... | |
| 6 | | Paraxial | רופאים | 0.000... | | -14.9253730 | | 12.5000000 U | - | - | - | 0.0000... | 1 |
| 7 | | Standard | Infinity | 0.000... | | | | 10.5011093 | 0.00... | 10.5011093 | 0.00... | 0.0000... | |
| 8 | (aper) | Standard | CORNEA | 7.800... | 0.520... | CORNEA | | 6.0000000 U | 0.00... | 6.0000000 | -0.5... | - | |
| 9 | (aper) | Standard | | 6.700... | 1.500... | AQUEO... | | 6.0000000 U | 0.00... | 6.0000000 | -0.3... | - | |
| 10 | | Standard | | 11.00... | 1.600... | AQUEO... | | 11.0000000 U | 0.00... | 11.0000000 | 0.00... | - | |
| 11 | | Standard | IRIS | Infinity | 1.000... | AQUEO... | | 4.0000000 U | 0.00... | 4.0000000 | 0.00... | - | |
| 12 | (aper) | Standard | LENS | 10.00... | 3.700... | LENS | | 5.0000000 U | 0.00... | 5.0000000 | 0.00... | - | |
| 13 | (aper) | Standard | | -6.00... | 0.000... | VITREOUS | | 5.0000000 U | 0.00... | 5.0000000 | -3.2... | - | |
| 14 | | Standard | | Infinity | 16.58... T | VITREOUS P | | 10.0002370 | 0.00... | 11.0000000 | 0.00... | - | |
| 15 | IMAGE | Standard | RETINA | -11.0... | - | | | 11.0000000 U | 0.00... | 11.0000000 | 0.00... | 0.0000... | |

Fig. 4

The properties – index of refraction, curvature and Abbe number - of the layers of the eye are summarized in the following table:

| Material | n_i | Abbe V_i | Abbe \tilde{V}_i | R_i |
|----------|-------------|-------------|--------------------|--------|
| Air | 1 | 0 | 0 | - |
| Cornea | 1.376980788 | 56.27993568 | 22.33330780 | 0.0078 |
| Aqueous | 1.336981204 | 52.65899113 | 20.89642505 | 0.0067 |
| Lens | 1.419976226 | 51.22614152 | 20.32783393 | 0.01 |
| Vitreous | 1.335981838 | 53.34217335 | 21.16752910 | -0.006 |

Table 2

It was found that the distance between the ophthalmic lens and the auxiliary lens varied depending on the shape of the lens placement and did not depend on the measured wavelength.

The auxiliary ray cone lens (in orange) simulates the propagation of the rays from the device. Additionally, we positioned the lens in the eye and the retina in a way that they see the rays in their true form as they are in the eye. In Fig. 5 the cone is seen to focus on the cornea (before being refracted).

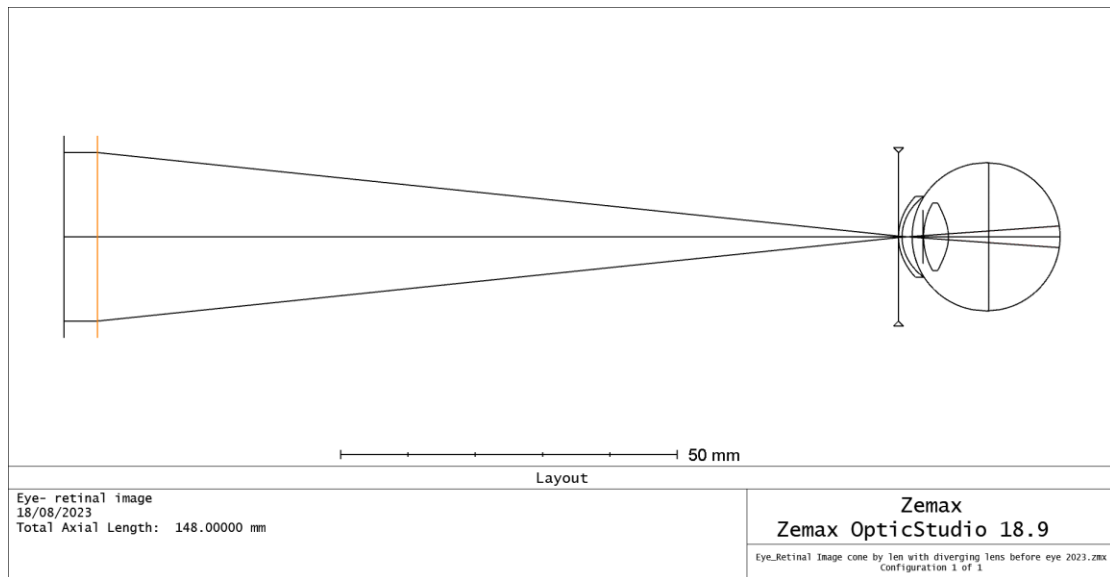


Fig. 5

The iris was defined with a Clear Semi-Diameter value of 4mm, making it similar to a maximum pupil size of 8mm, which is achieved through pupil dilation using eye-drops. Thus, even when focusing on the retina, one observes that the entire beam width will pass through the iris (in orange).

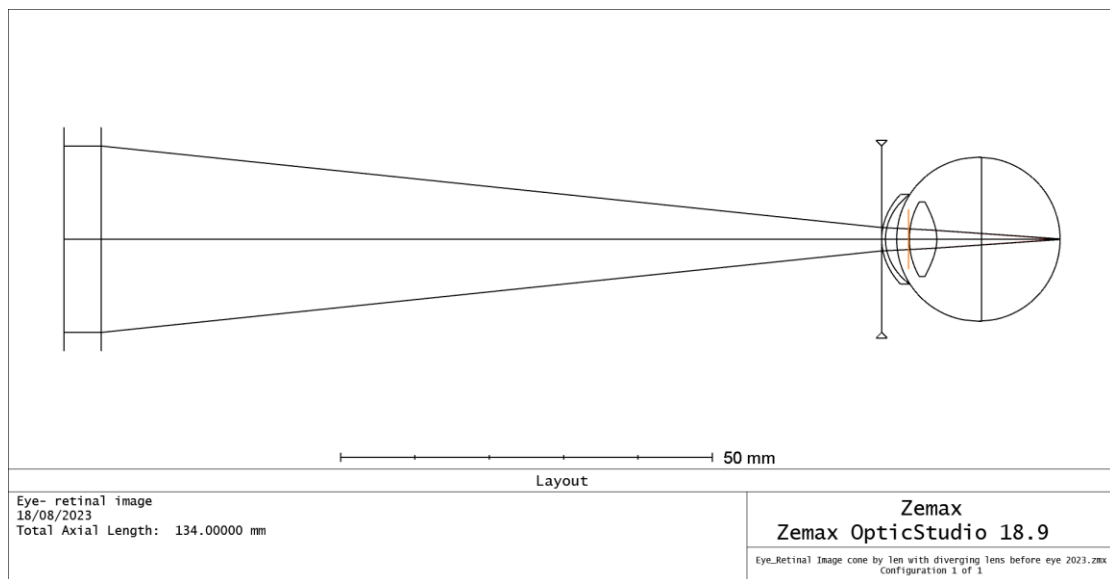


Fig. 6

At this stage, we began adjusting the simulation plane within the eye, from the eye's lens to the cornea. We performed optimization at each position, ensuring that the rays of direction (in red) are captured on this plane. This simulation mirrors what medical professionals observe in relation to the treatment outcome achieved in reality.

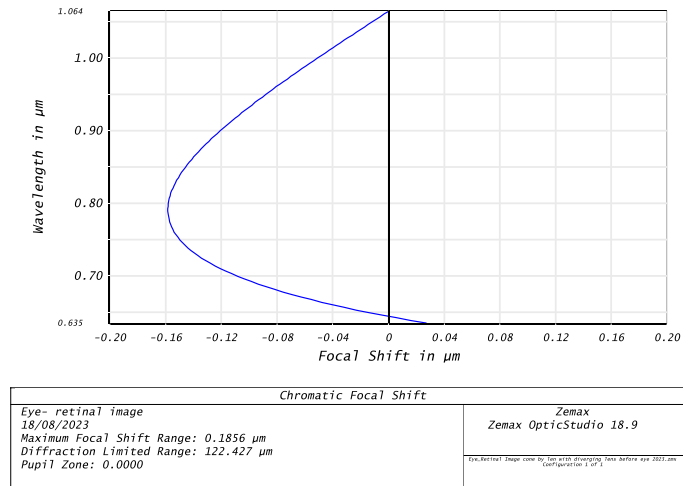


Fig. 7

Deviation in millimeters: 0.00002730.

At a depth of 7.42 mm within the eye, adjacent to the eye's lens, we observed that the treatment beam focuses in front of the guide-beams.

At a depth of 8 mm, we achieved almost complete convergence between the rays:

At a depth of 8.5 mm within the eye, a deviation between the rays began, but in the opposite direction. The treatment beam focused beyond the convergence point of the rays of direction, resulting in the following outcome:

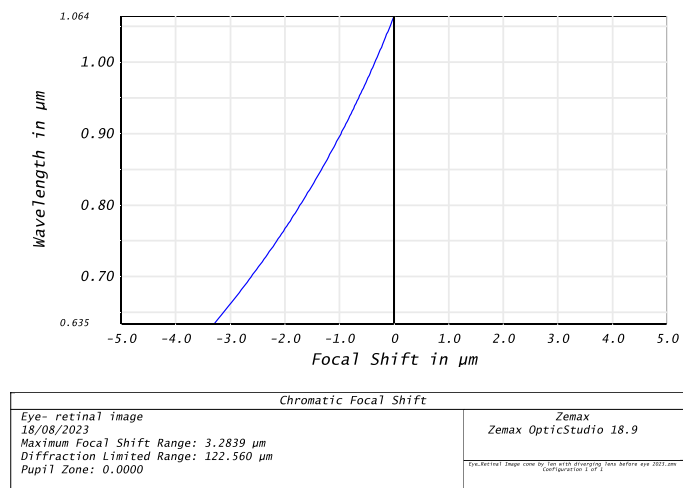


Fig. 8

Deviation in millimeters: 0.00328388.

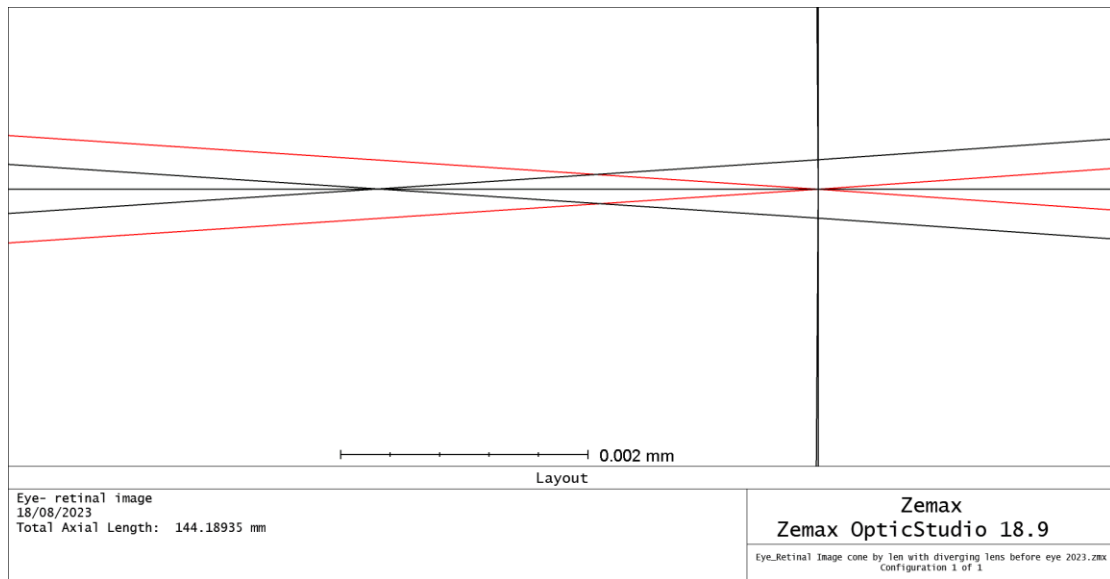


Fig. 9

At a depth of 23.67 mm, we observed a significant deviation in the treatment beam, which now intersects with the retina:

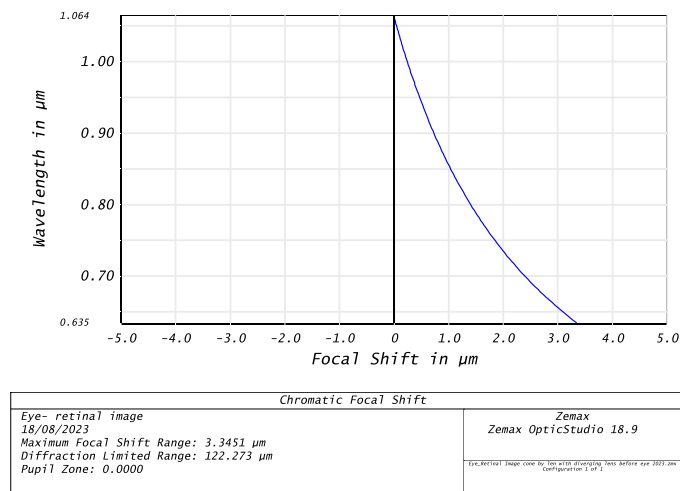


Fig. 10

Deviation in millimeters: 0.00334510.

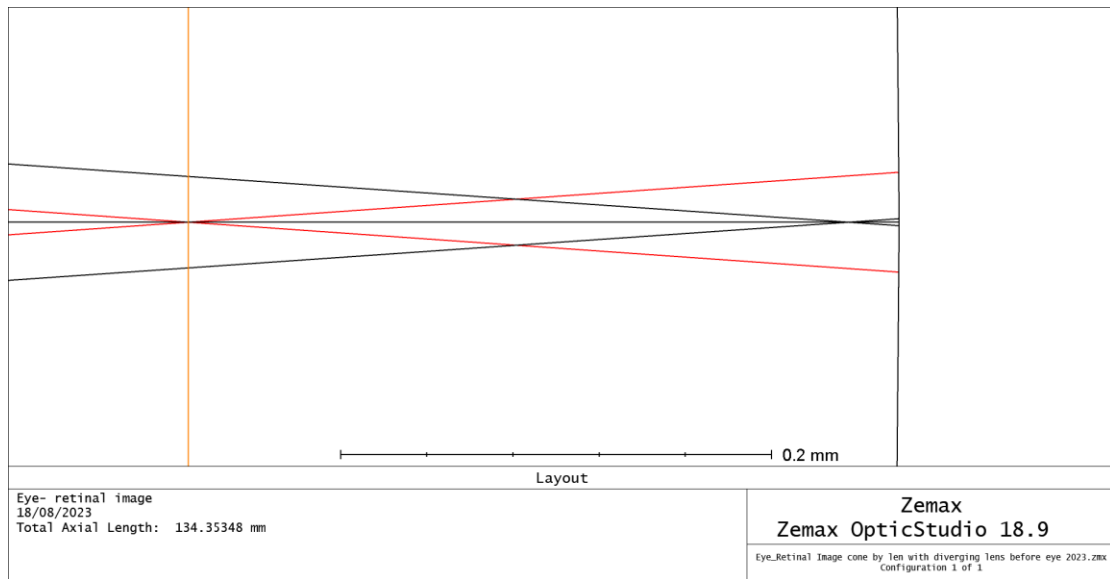


Fig. 11

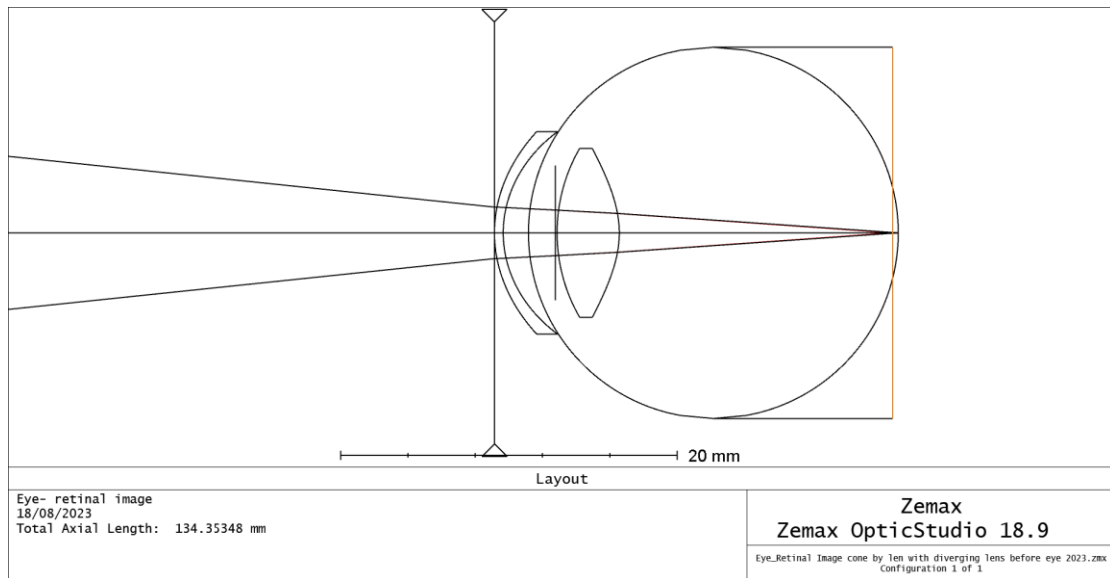


Fig. 12

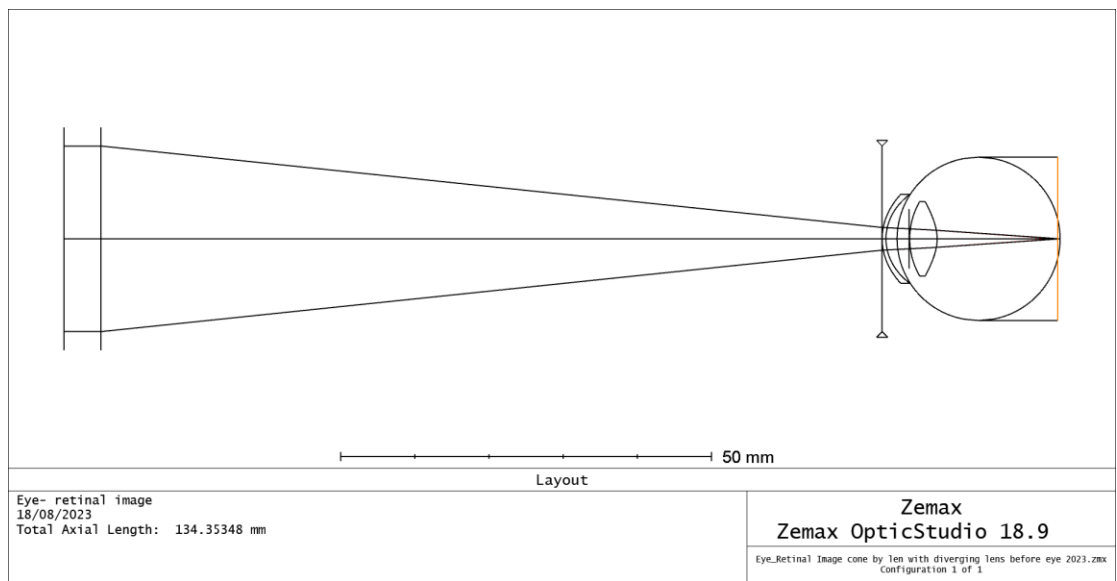


Fig. 13

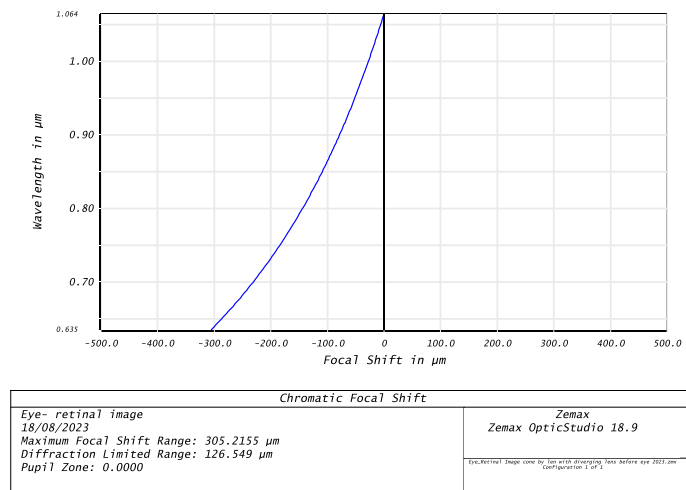


Fig. 14

Deviation in millimeters: 0.30521550.

4. Relative deviation between guide-beam and treatment-beam foci switches sign. In (Fig. 16) the guide-beams (in red) focus before the treatment beam. In (Fig. 15) the guide beams focus after the treatment beam.

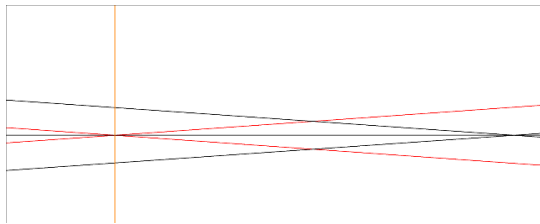


Fig. 16

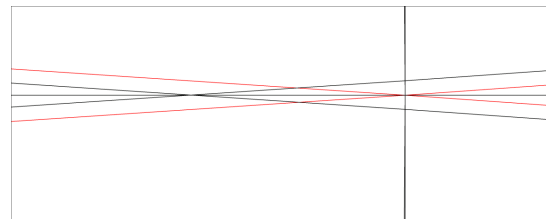


Fig. 15

5. Modeling of Light Cone with ZOS In (Fig. 17) the light cone focuses on the front of the cornea. The light cone focuses near the retina (Fig. 18).

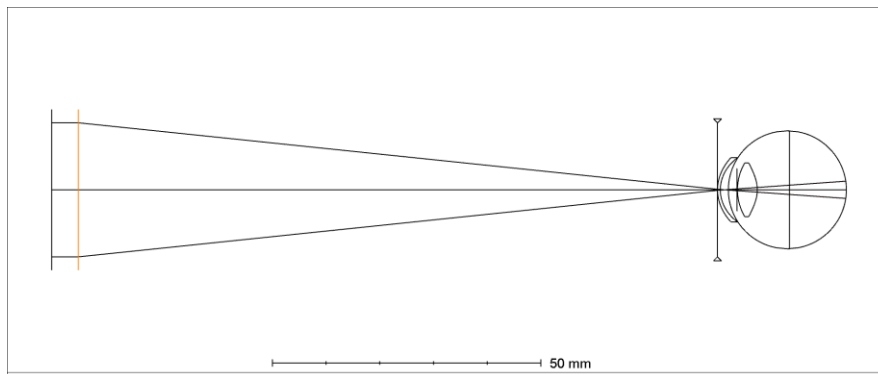


Fig. 17

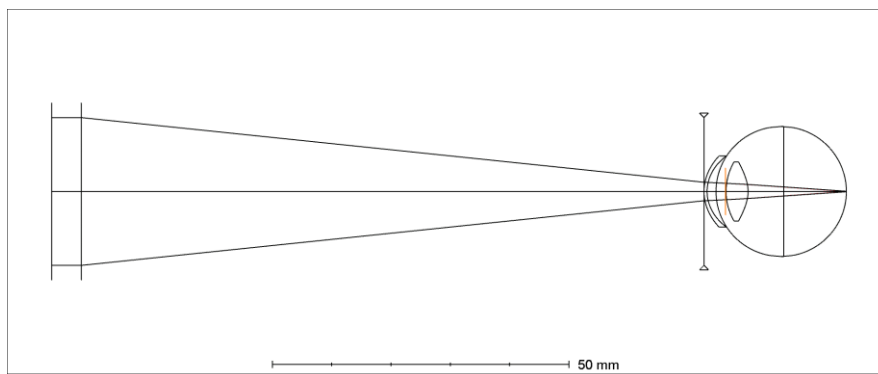


Fig. 18

We compiled all the deviations into a table and graph, and summarized the data as follows:

| Focusing at the depth within the eye [in mm] | Deviation in the eye [in microns] |
|---|--|
| 7.42 | -3.3451 |
| 8 | -0.0273 |
| 8.5 | 3.28388 |
| 9 | 7.01303 |
| 10 | 15.72672 |
| 11 | 26.11689 |
| 12 | 38.18696 |
| 13 | 51.94074 |
| 14 | 67.38252 |
| 15 | 84.51722 |
| 16 | 103.35047 |
| 17 | 123.88879 |
| 18 | 146.13978 |
| 19 | 170.11229 |
| 20 | 195.81671 |
| 21 | 223.26525 |
| 22 | 252.47222 |
| 23 | 283.45448 |
| 23.67 | 305.2155 |

Table 3

6. Device Calibration

The Melos 500 device allows for measurements of lens focal lengths, but due to its prolonged period of inactivity, it presented several challenges.

- a. **Device Calibration:** The device was disassembled, and its components were cleaned from accumulated dust. Its operational principle was restored, and the burnt-out light source was replaced with a temporary one. The distances were adjusted to obtain a focused image.
- b. **Eyepiece Alignment:** Over time, the working distance between the eyepiece and the glass plate had changed. When the image of the grids appeared in focus, the scale became blurred, or vice versa. A correction was made so that the eyepiece's focus aligned with the marked glass plate.
- c. **Measurement Scale:** The length of the scale, marked with 250 divisions, was measured, and found to be one centimeter.
- d. **Magnification Factor:** Since the device's specifications did not provide the focal length of the collimator lens f_k or the size of the object y , it was not possible to directly convert the measured image length (in divisions) to the focal length of the demonstrated lens. Therefore, a conversion factor was defined as $\frac{f_k}{y} = 2.667_{\text{cm/ruling}}$, as explained in Appendix 8.

7. Performing Measurements with the Device

After obtaining the conversion factor, the device was used to characterize the focal length of the lens in this manner.

A measurement was conducted using a supplementary lens attached to the physician's lens. A green-filtered light source was used, and 16 squares were observed within the range of 100 to 105 (Fig. 19 The grids for the auxiliary). According to the conversion factor formula, $y' = \frac{5}{16}$ was obtained. By multiplying this value by the conversion factor, the focal length was calculated as $= 2.667 \cdot \frac{5}{16} = 0.83 \pm 0.05_{\text{cm}}$. Another measurement was performed using white light as the light source without the filter. It showed 15 squares within the same range obtained from the previous measurement. According to the equations derived, the focal length was calculated as $f = 2.667 \cdot \frac{5}{15} = 0.88 \pm 0.05_{\text{cm}}$. After obtaining a value close to the auxiliary lens, it was connected to the physician's lens, resulting in 11 squares within a range of 2 units (Fig. 20 The grids for both lenses). Again, using the conversion factor, the common focal length for both lenses was calculated as $f = 2.667 \cdot \frac{2}{11} = 0.48 \pm 0.05_{\text{cm}}$. Using the lens

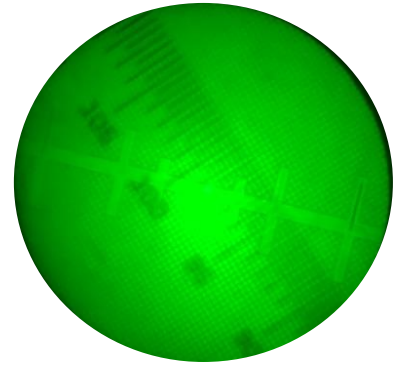


Fig. 19 The grids for the auxiliary

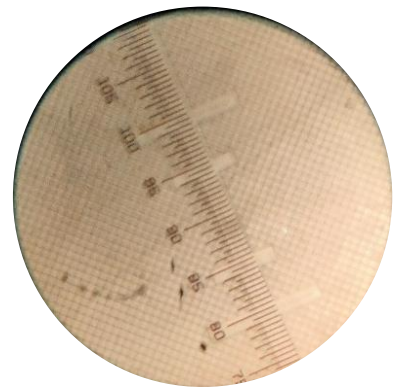


Fig. 20 The grids for both lenses

combination equation, the lens's value could be calculated: $\frac{1}{f} + \frac{1}{0.83} = \frac{1}{0.48} \rightarrow f = -1.13269_{cm}$. Hence, the focal power of the scattering lens is -88.49 diopters.

8. Using the Melos 500 the focal length of the lens, f_p , was derived from the size of the formed image using the following equation:

$$f_p = \frac{f_k}{y} y',$$

in which y is the actual size of the square, y' is the size of the square as measured in the image, and f_k is the distance between the object and the collimator lens, which represents the focal point.

To determine the conversion coefficient, $\frac{f_k}{y}$, we measured the image size for the two lenses with a known focal length (2 cm and 10 cm), and the conversion coefficient was defined as 2.667 cm/ruling as follows:

$$\frac{f_k}{y} = \frac{f_p}{y'} = \frac{10_{cm}}{3.75} = 2.667_{cm/ruling}$$

$$\frac{f_k}{y} = \frac{f_p}{y'} = \frac{2_{cm}}{0.75} = 2.667_{cm/ruling}$$

Using this conversion coefficient, we can measure the focal length of any diverging lens, including the Volk Goldmann 3-mirror lens we used in our study.

9. Rays Focused on the Center of Curvature are not Refracted

Rays focused on the center-of-curvature of concentric eye surfaces are incident perpendicularly. Thus the rays experience no refraction.

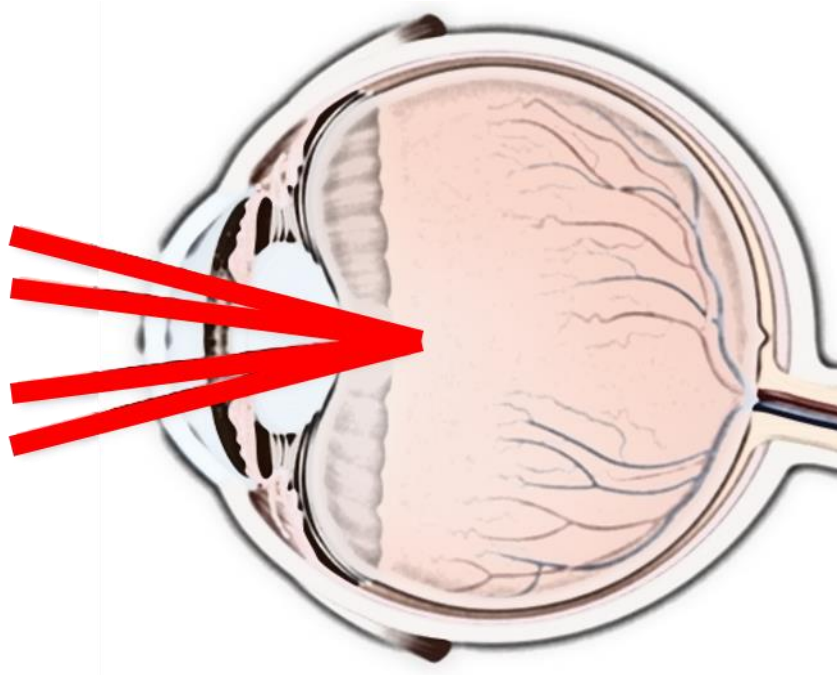


Fig. 21

10. The spectral output of wavelengths in the autocollimation system.

In order to obtain the focal length of the ophthalmologist lens, measurements were taken at various wavelengths. The spectral output for each wavelength from the measured waves is presented in Figures 4-6.

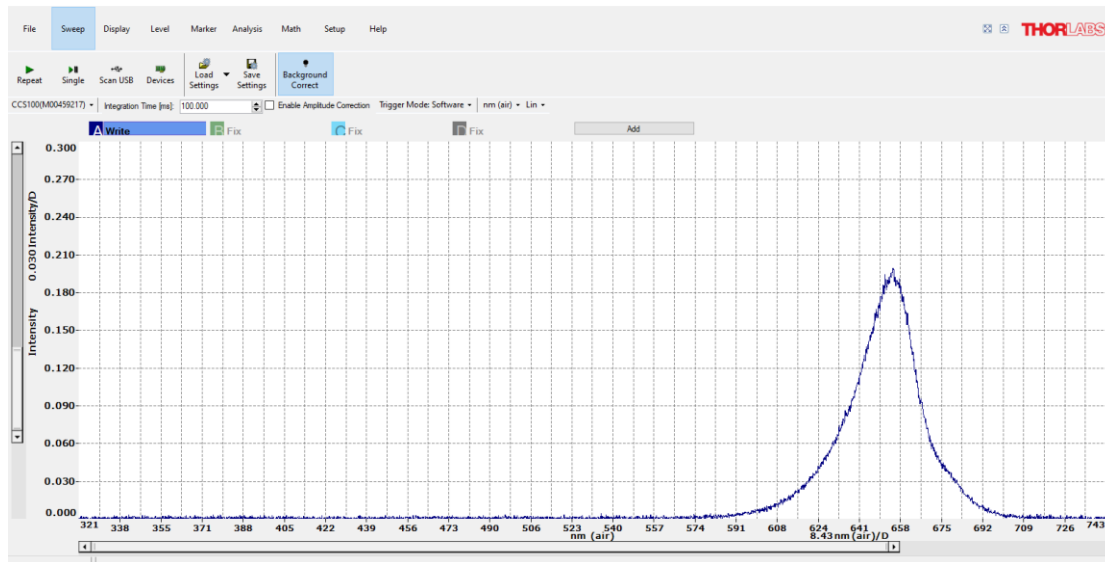


Fig. 22 Spectral output of red LED

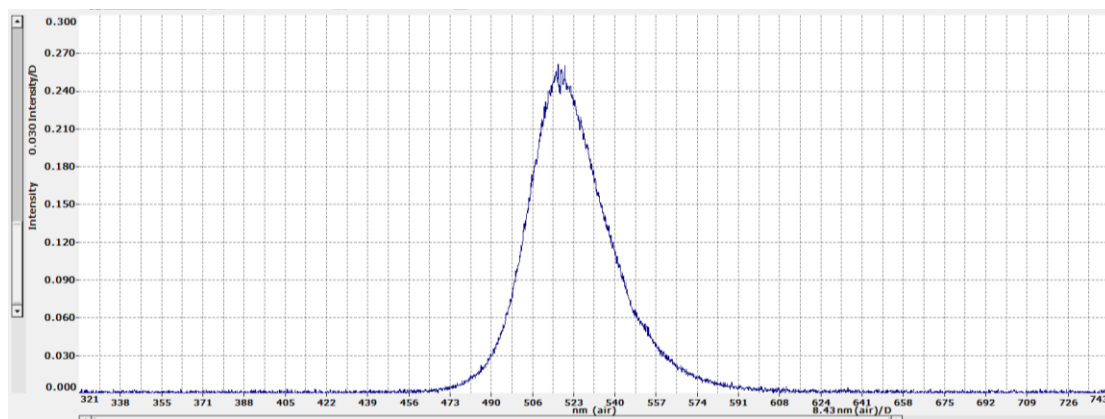


Fig. 23 Spectral output of green LED

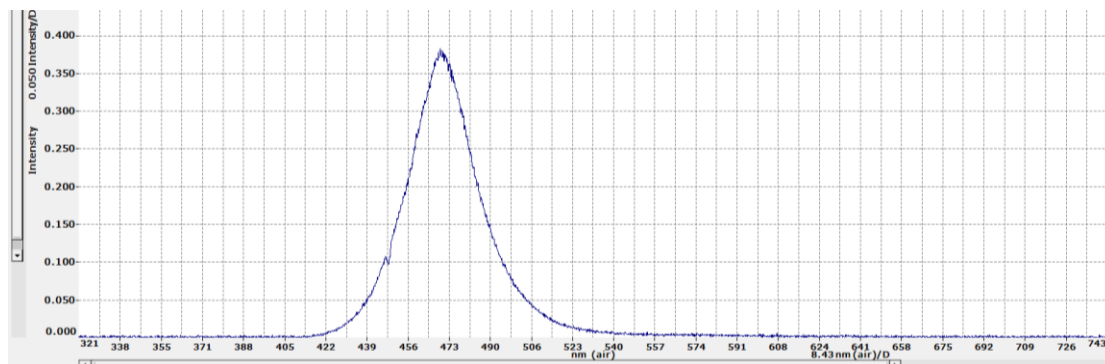


Fig. 24 Spectral output of blue LED